International Journal of Disaster Risk Reduction 76 (2022) 103002

Contents lists available at ScienceDirect

International Journal of Disaster Risk Reduction

journal homepage: www.elsevier.com/locate/ijdrr

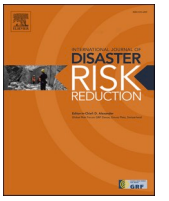

Relative seismic and tsunami risk assessment for Stromboli Island (Italy)

Agnese Turchi [a,*], Federico Di Traglia [b], Roberto Gentile [c], Alessandro Fornaciai [d], Iacopo Zetti [e], Riccardo Fanti [f]

[a] Department of Architecture, PLINIVS-LUPT Study Centre, University of Naples Federico II, Via Toledo 402, 80134, Naples, Italy
[b] Istituto Nazionale di Oceanografia e di Geofisica Sperimentale – OGS, Borgo Grotta Gigante 42/C, 34010, Sgonico, Italy
[c] Institute for Risk and Disaster Reduction, University College London, WC1E 6BT, London, United Kingdom
[d] Istituto Nazionale di Geofisica e Vulcanologia, Sezione di Pisa, Via Cesare Battisti 53, 56125, Pisa, Italy
[e] Department of Architecture, University of Florence, Via Micheli 2, 50121, Florence (FI), Italy
[f] Department of Earth Sciences, University of Florence, Via La Pira 4, 50121, Florence (FI), Italy

ARTICLE INFO

Keywords:
Relative risk assessment
Seismic risk
Tsunami risk
Volcanic islands
Stromboli
Aeolian archipelago

ABSTRACT

An innovative method of estimating the relative risk of buildings exposed to seismic and tsunami hazards in volcanic islands is applied to Stromboli (Italy), a well-known stratovolcano affected by moderate earthquakes and mass-flow-induced tsunamis. The method uses a pre-existing quali-quantitative analysis to assess the relative risk indices of buildings, which provide comparative results useful for prioritisation purposes, in combination with a historical-geographical settlement analysis consistent with the 'territorialist' approach to the urban and regional planning and design. The quali-quantitative analysis is based on a new proposed survey-sheet model, useful to collect building information necessary for the relative risk estimation, whereas the historical-geographical investigation is based on the multi-temporal comparison of aerial and satellite images. The proposal to combine two consolidated methods represents an innovation in estimating relative risk. Considering that Stromboli Island had never been subjected to similar analyses, the results of the relative seismic risk assessment are novel and moreover identify buildings with a fairly-low and spatially-uniform relative risk. The results of the relative tsunami risk assessment are consistent with results of similar past studies, identifying buildings with a higher relative risk index on the northern coast of the island. The combined use of a building-by-building survey with a multi-temporal analysis of settlements allows obtaining a higher detail than previously available for the region. If adequately modified, the proposed combination of methods allows assessing relative risk also considering other geo-environmental hazards and their cascading effects, in a multi-hazard risk assessment perspective.

1. Introduction

Volcanic areas can be prone to non-eruptive hazards such as earthquakes, landslides, and floods. In addition, coastal and island volcanoes can also be subject to tsunamis usually generated by mass-flows (e.g., landslides or pyroclastic density currents, PDCs) that

* Corresponding author.
E-mail addresses: agnese.turchi@unina.it (A. Turchi), fditraglia@ogs.it (F. Di Traglia), r.gentile@ucl.ac.uk (R. Gentile), alessandro.fornaciai@ingv.it (A. Fornaciai), iacopo.zetti@unifi.it (I. Zetti), riccardo.fanti@unifi.it (R. Fanti).

https://doi.org/10.1016/j.ijdrr.2022.103002
Received 26 January 2022; Received in revised form 24 April 2022; Accepted 25 April 2022
Available online 29 April 2022

impact the sea, underwater explosions, or caldera collapses.

In this work, an innovative method for estimating the relative risk of the elements (i.e., buildings) exposed to seismic and tsunami hazards on volcanic islands is proposed. The procedure uses an already consolidated quali-quantitative analysis method for the assessment of building relative risk using indices (i.e., [16,17,32], which allow comparing the risk of different buildings, although not providing reliable absolute estimations of it. This is combined with the historical-geographical analysis of urban and extra-urban settlements, based on the multi-temporal comparison of aerial and satellite images, taken from the 'territorialist' approach to the urban and regional planning and design (according to Refs. [42–44]. The aim is to obtain a relative risk-based prioritisation assessment as accurately as possible, through methods never used in a complementary way, to prevent and mitigate geo-environmental risks.

The 921 m high Stromboli Island (Italy), located in the South Tyrrhenian Sea (Fig. 1), is the emerging part of a ~3000 m high, slightly NE-SW elongated stratovolcano [63]. The frequency of the hazards that affect the island, the number of documents about the damage due to these hazards, and the geographical and architectural characteristics of the assets make Stromboli an optimal case study to test the procedure.

The risk related to seismic phenomena is quite ignored on the island compared to volcanic phenomena, such as the explosive (e.g., Ref. [9] and effusive (e.g., Refs. [21,22] eruptions and tsunamis (e.g., Ref. [25]. Indeed, historical chronicles and earthquakes catalogs highlight that the island suffered the impacts of numerous seismic events (i.e., [12,26,37,51], even in the recent years (the early 1900s and 1960s). As a consequence, also the seismic risk on Stromboli Island must be considered.

On the contrary, analysing tsunami risk on Stromboli is paramount, being the island affected by mass-flow-induced tsunamis with an average of 1 event every 20 years [45]. Consequently, the Italian Civil Protection Department defined an alert and emergency plan that identifies tsunamis as one of the main risks for the population [57].

Moreover, Stromboli is a case study that allows the validation of the adopted models using physical damage data collected in situ, after seismic and/or tsunami events (i.e., ground-truth), and reported in several works already published (i.e., [12,64,65].

Finally, the selected case study shows a modest surface extension and a few elements potentially exposed to seismic and tsunami hazards. Therefore, it can be considered a suitable case study for collecting a large amount of information about the main characteristics of buildings and for developing analyses at a local scale, maintaining a general overview of the territorial context.

The choice of using intermediate scales (i.e., 1:10000, 1:5000, and 1:2000) and a quali-quantitative approach for the assessment of building relative risk involved the creation of a comprehensive survey-sheet model (e.g., Refs. [23,47,58,59,75], and reference therein; [16,24,32,48,76], useful for building-by-building surveys. The process to calibrate the survey-sheet model also took into consideration the local characteristics of buildings, deriving from unstructured interviews with some workers in the construction sector (i.e., bricklayers) on the island. At the same time 'territorialist' analysis (according to Refs. [42–44], based on the multi-temporal comparison of aerial and satellite images, allowed to better estimate some attributes of buildings as the construction period which, in turn, is directly related to the building typologies, function, and construction materials and techniques.

2. The Stromboli Island

2.1. Seismic hazard

At Stromboli, apart from the seismic signature of the volcanic activity (i.e., tremor, very long-period earthquakes, and explosion

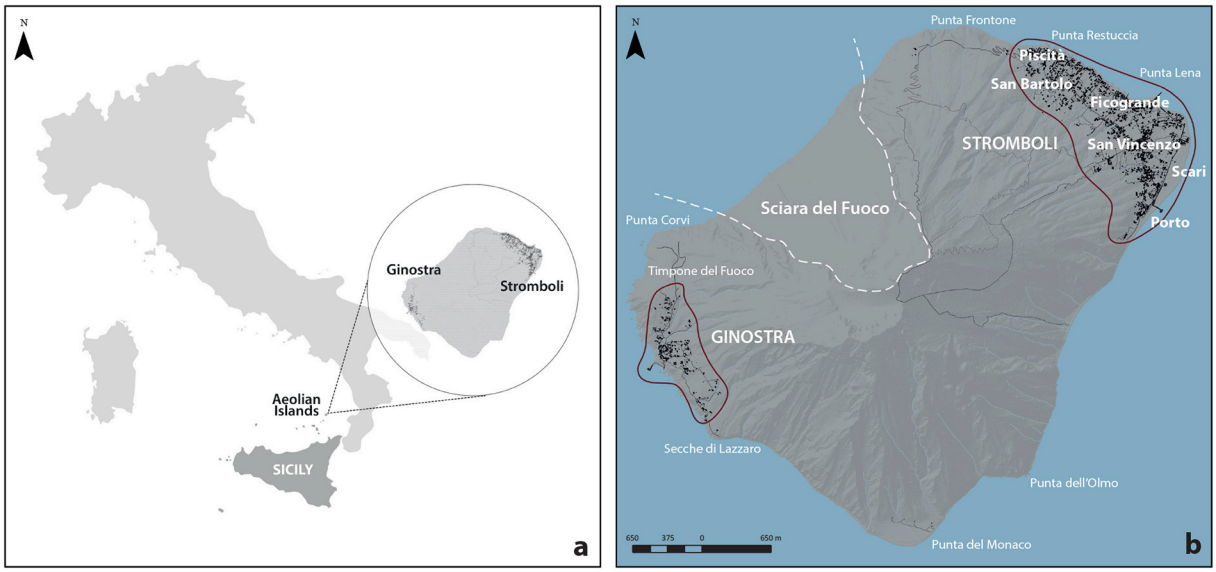

Fig. 1. Geographical location of the study area: a) Stromboli is one of the seven islands (i.e., Alicudi, Filicudi, Salina, Lipari, Vulcano, Panarea, and Stromboli) of the Aeolian archipelago (Municipality of Lipari in Messina Province, Sicily Region, Italy); b) Stromboli village is located on the north-eastern side of the island, while Ginostra is located on the western side.

quakes; [26], tectonic earthquakes associated with brittle failure of rocks were rarely recorded [15,69,72]. Falsaperla & Spampinato [26] resumed the tectonic seismicity in Stromboli from 1885 to 1999, considering crustal earthquakes having minimum intensity in the Mercalli-Cancani-Sieberg scale (MCS) equal to IV. There were 182 earthquakes in 91 years, with only four events having MCS intensity $\geq$ VIII. By refining the analysis conducted by these authors, the Italian Macroseismic Database [37]; Table S2 in supplementary material) provides a homogeneous set of macroseismic intensities from different sources relating to earthquakes with maximum intensity $\geq$5 in the time interval 1000–2017 A.D. In this way, it is possible to identify 43 events, of which 10 of I $\geq$ 6 on Stromboli Island. Among these, 4 originated in the Calabrian arc (i.e., 1783, 1894, 1905, 1928), 1 in the Strait of Messina (i.e., 1908) and the remaining 5 had their epicentre located around Stromboli (i.e., 1888, 1909, 1916, 1941, 1969). Details on the local effects of seismic events can be found in some historical chronicles. For example, referring to the earthquake of 25th February 1888, with its epicentre in Stromboli, local effects were reported, such as ground-shaking widely perceived in the inhabited area, damage to the vault of the church, damage to the walls of the houses, the collapse of sea-cliffs, the fractures in the ground, no casualties. The description of the effects of the earthquake of 16th November 1894, which took place in the Calabria Region and Sicily Region, was made by Riccò [51] that reported damage to the San Vincenzo church in the village of Stromboli (i.e., fractures in the walls; breaking of the keys of the vaults; damage to the bell towers). The church was already destroyed and rebuilt after previous earthquakes. The San Bartolomeo church was completely damaged by previous earthquakes and was rebuilt at the time of the 1894 earthquake.Moreover, all the houses in Stromboli had injuries, more serious in all those with two floors and poorer or older in terms of construction period. Also in houses with iron chains, large fractures occurred, and several cisterns have cracked. The last earthquake of considerable intensity (i.e., I = 6) occurred in Stromboli on 16th April 1960 [12]. There was panic among the population and a high level of damage was recorded to the houses and also to the churches of San Vincenzo and San Bartolo. The macroseismic data collected by Cavallaro [12]; reported greater effects in the Stromboli village (especially in the area of San Vincenzo church), and minor effects in the Ginostra village.

Stromboli is not only affected by local seismicity but also by earthquakes that occur in Sicily and Calabria Regions. The peak ground acceleration (PGA) values proposed by the National Institute of Geophysics and Volcanology (INGV – Istituto Nazionale di Geofisica e Vulcanologia), which is between 0.175 g and 0.225 g [61]; http://esse1-gis.mi.ingv.it/), represents the only contribution of the seismicity of distant origin. Therefore, they cannot be considered fully representative. According to its tectonic setting, Stromboli is not comparable with the central islands of the Aeolian archipelago (i.e., Lipari, Vulcano, and Salina). The PGA values recalculated for Stromboli are reported in Table 1:

2.2. Tsunami hazard

The mass-flows triggering tsunami at Stromboli can be either landslides of unstable slopes (mainly on the NW sector of the island, locally called Sciara del Fuoco, a steep and unstable slope constantly filled by unconsolidated deposits and/or lava flow) or PDCs. Due to its persistent volcanic activity and the dynamic of the Sciara del Fuoco, Stromboli is one of the main sites in the Mediterranean Sea where non-earthquakes-induced tsunamis can be generated.

The Stromboli volcano was affected by several flank collapse events, both in its SE and NW flanks [11,36,53,62,70]. Two notable flank collapse events of the Sciara del Fuoco, which were associated with highly explosive events and water-magma interaction, were recognized in the geological record [33,39,52]. The youngest occurred between 7-4ka (i.e., Neostromboli products) and A.D. 45–245 (i.e., 380-100 BC, Pizzo products). This event is likely associated with the so-called Semaforo Labronzo hydromagmatic eruption [31, 39]. An older collapse occurred 6.7–6.2ka [52] in association with the Secche di Lazzaro hydromagmatic eruption [4,49]. Another recent massive landslide, which most likely occurred in the 14th century [3,60], produced a submarine turbidite deposit [18], and it could be connected with tsunamis that had significant impacts both on the island of Stromboli and on the whole South Tyrrhenian coasts [50,54].

Present-day mass-wasting phenomena at Stromboli, mainly located within the NW and SE flank, vary from small rockfall and gravel flows (i.e., $<10^6$ m^3) to rockslides/rock avalanches (i.e., 10^6–$10^7$$m^3$), up to deep-seated gravitational slope deformations that evolve into debris/rock avalanches (i.e., $>10^7$ m^3), typical of sectoral collapse events [20]. The most recent landslide of notable importance (i.e., 25-30 $\times$ 10^6 m^3) [13,67] occurred on 30th December 2002 [1,8] and caused a tsunami sequence with a maximum run-up of about 11 m at the Stromboli village [66]. Tsunamis also occurred in recent times as in 1879, 1916, 1919, 1930, 1944, and 1954 [45]; Table S1 in supplementary material). Recently, three well-preserved medieval tsunami deposits were identified on the north-eastern coast of the island [50,54] which, together with the data on tsunamis that occurred in the 20th and 21st centuries, indicate a high frequency of tsunamis associated with eruptive events and plausibly with landslides in the Sciara del Fuoco. Although the mechanism by which Stromboli triggers tsunamis is poorly understood, all known tsunamis were generated during periods of intense volcanic activity and therefore, a link between the tsunami trigger and increased volcanic activity is at least plausible. Historical events reveal that the possible mechanisms of tsunami generation are i) submarine landslides which, in turn, are triggered by flank destabilization induced by magma intrusions or material accumulations (as in 2002; [1] or ii) PDCs produced by paroxysmal explosions (as in 1930; [19]. No eyewitness accounts, nor reconstruction using numerical models, report that in Stromboli there were significant effects of the tsunamis generated by regional earthquakes with sources in the Calabria Region or Sicily Region (e.g., Refs. [38,56].

Table 1
500-year return period PGA [g] estimated for Stromboli Island [61]; http://esse1-gis.mi.ingv.it/).

Site	Longitude	Latitude	a_{max} (50th percentile)	a_{max} (84th percentile)
Stromboli	15.2204	38.8214	0.1956	0.2290
	15.2191	38.7714	0.2024	0.2391

An assessment of the probabilistic tsunami occurrence on Stromboli Island is missing. Different tsunami waves generation and propagation were modelled, considering different triggering scenarios and models [28,29,65]. The results of a recent one, made by Fornaciai et al. [29]; were considered here to define different intensity scenarios and to assess the relative tsunami risk of the exposed

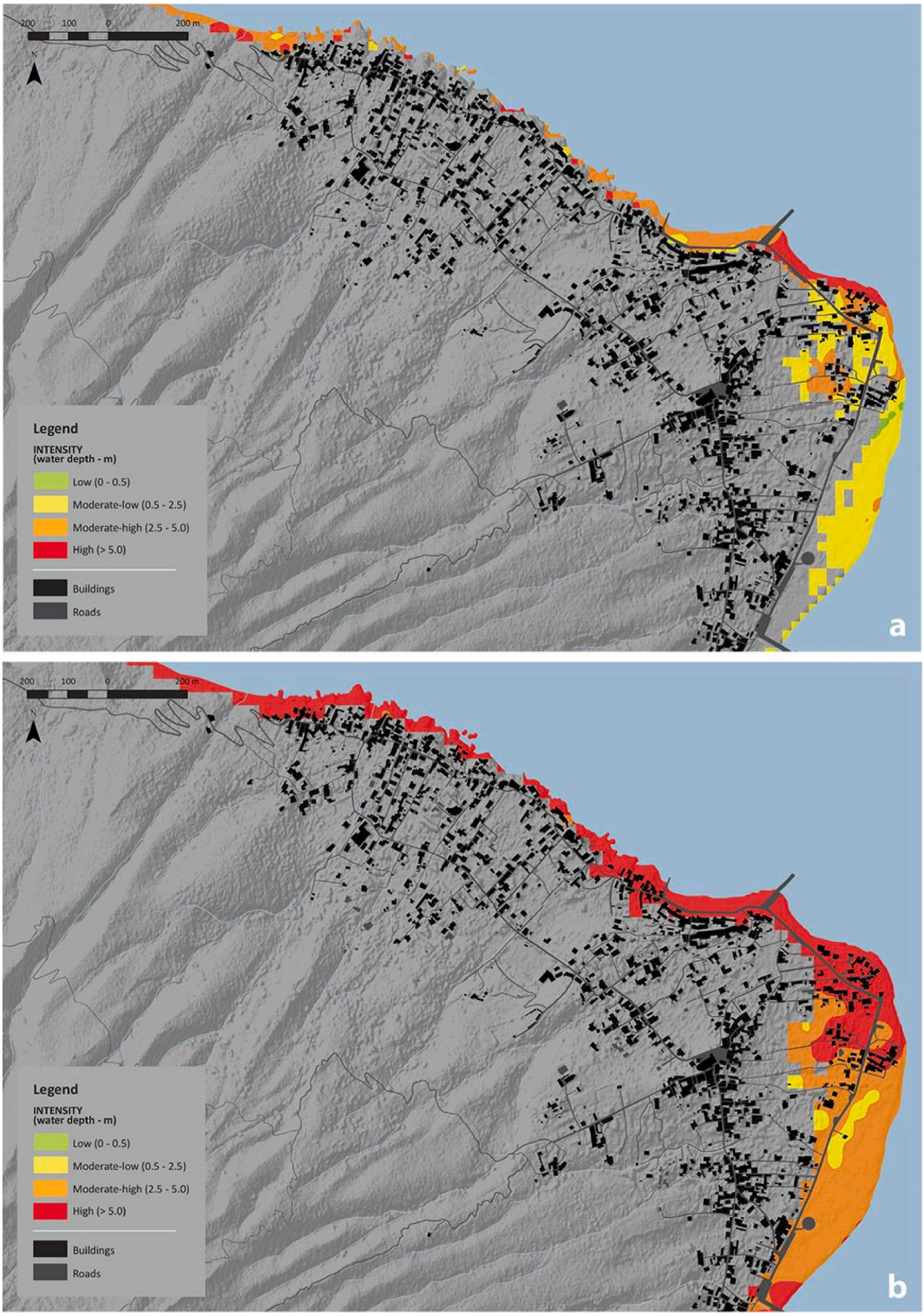

Fig. 2. Tsunami intensity in Stromboli village: a) scenario 1 (submarine landslide, 17.5×10^6 m^3) and b) scenario 2 (subaerial landslide, 35.3×10^6 m^3).

elements. Fornaciai et al. [28,29] simulated tsunami waves generated by landslides in the Sciara del Fuoco, through NHWAVE numerical models [40,41], a model able to simulate tsunami triggers, wave propagation, run-up, and inundation on the island. These authors simulated eight different scenarios triggered by submarine landslides with a volume of 7.1, 11.8, 17.6, and 23.5 $\times$ 10^6 m^3 and subaerial landslides with a volume of 4.7, 7.1, 11.8, and 35.3 $\times$ 10^6 m^3. In this work two scenarios were taken into account:

- scenario 1, related to a 17.6 $\times$ 10^6 m^3 submarine landslide (Fig. S1a in the supplementary material; Fig. 2a) and considered by Fornaciai et al. [29] as representative of the 30th December 2002 event [67];
- scenario 2, related to a 35.3 $\times$ 10^6 m^3 subaerial landslide (Fig. S1b in the supplementary material; Fig. 2b) which was the largest scenario simulated by Fornaciai et al. [29]; estimated to occur in tens to hundreds of years by Schaefer et al. [55].

Tsunami scenarios 1 and 2 were used for calculating the tsunami intensity on the island. Tsunami intensity depends on water depth above the terrain level, resulting from the difference between the wave height derived from the results of simulations and the elevation obtained from a digital elevation model (DEM) of the Island. For the latter, a Light Detection and Ranging (LiDAR) DEM with 1-m resolution was used (instrumental vertical and horizontal accuracy of 0.10–0.20 m and 0.25 m; see Ref. [21]. The LiDAR DEM was resampled to 30 m resolution to make it equivalent to the model-derived wave height maps.

3. Materials and methods

3.1. Creating a new survey-sheet model

As widely described in the relevant scientific literature (e.g., Refs. [23,47,58,59,75] and reference therein; [16,24,32,48,76], in order to assess the building relative risk to one or more geo-environmental hazard, it is necessary to collect information relating to the main relevant compositional characteristics of the elements.

The proper instrument used to create an accurate and efficient database is the survey-sheet, which allows both detailed and more-rapid surveys. The survey-sheet model is usually calibrated for building-by-building data collection, in relation to some main variables like the scale of analysis (e.g., national, interregional, regional, sub-regional, municipal, local, etc.), surface extension of the study area, type of hazard that affects the study area, morpho-typological characteristics of the anthropic settlements, number of buildings potentially exposed, time available to collect data, and methodological approach used for the relative risk assessment (e.g., quantitative, quali-quantitative, qualitative, etc.). Therefore, the structure of the model can remarkably vary case by case.

According to the geographical characteristics of Stromboli Island, the proposed survey-sheet model (Figs. S2 and S3, in the supplementary material) was created to allow rapid surveys and, at the same time, to gather building-by-building information as detailed as possible, obtaining a complete and exhaustive database at a local scale.

The survey-sheet model was primarily obtained through the intersection of two pre-existing models: the AeDES sheet (i.e., [24] and the sheet made by the Department of Earth Sciences of the University of Florence (DST-UNIFI) (i.e., [48]. The first one, which is very detailed and focused on the peculiarities of structures, is commonly used by the Italian Civil Protection Department to collect information about the state of buildings after a seismic event. The second one, which is characterised by a multi-risk approach and focused not only on the structures but also on the surrounding environment, is used by the DST-UNIFI and National Institute for Insurance against Accidents at Work, Tuscany Region Directorate (INAIL – Istituto Nazionale per l'Assicurazione contro gli Infortuni sul Lavoro, Direzione Regionale Toscana) to analyse the vulnerability of buildings with strategic function of civil protection (e.g., schools). Secondarily, the survey-sheet model was designed and calibrated using a series of preliminary analyses focused on the geographical-historical evolution of urban and extra-urban settlements, based on multi-temporal analysis of orthophotos at several temporal thresholds (i.e., 1954 and 1974 aerial photographs, and 2019 PLÉIADES-1 satellite image in Fig. 3). This approach allows deeply knowing the peculiarities of the territory (i.e., [42–44] in terms of compositional characteristics (e.g., materials and local constructive techniques), permanences/persistences (e.g., typologies and functions), and transformation processes of the built

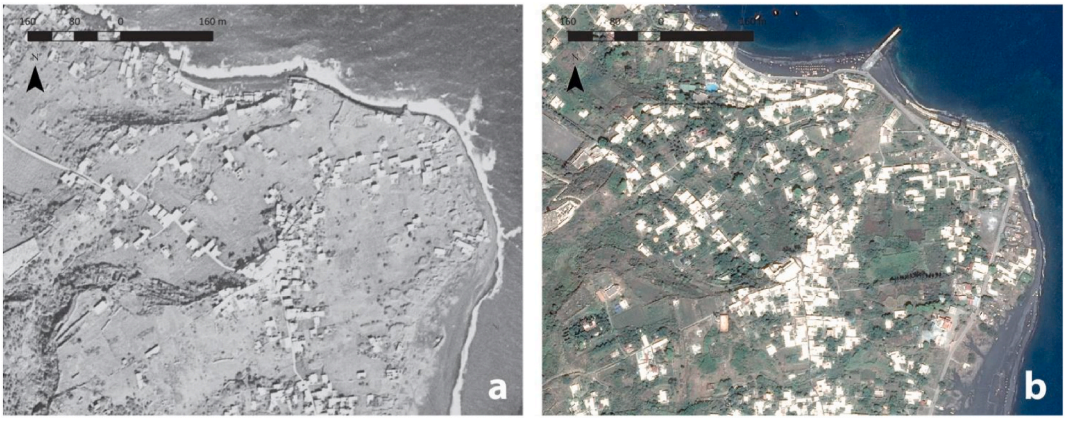

Fig. 3. Cartographic data used to analyse the transformation of the Strombolian territory: a) IGMI-G.A.I. orthophoto of 1954 (i.e., OFC 1954_10 k), and b) the most recent PLEIADÉS-1 satellite image of 8th October 2019 (i.e., PLEIADÉS-1 2019).

environment over time.

The new survey-sheet model is divided into two main complementary sections: the first one consists of general information aimed at retrieving ancillary yet important data on buildings and their surroundings, while the second one consists of all those specific information on compositional characteristics of buildings aimed at assessing the vulnerability of elements concerning the type of hazard that can occur in the study area.

The main *general information* (Fig. S2) that was identified and taken into account is: location (i.e., Stromboli or Ginostra), building representation on CTR, construction year, heritage value, building state (i.e., completed, under construction, or uncompleted), building maintenance (i.e., high quality, low quality, or abandoned), use of interior spaces (i.e., >65%, 30–65%, <30%, or unused), building function (i.e., residential, religious, tourist-receptive, commercial, service industry, or productive), building typology (i.e., Aeolian house, shed/veranda, canopy, oven, civil specialized building as school, barrack or semaforo marittimo/lighthouse, industrial specialized building as mills, religious specialized building as church/chapel, votive shrine, columbarium/tomb, or other), owner (i.e., public, private, or public-private), strategic function for civil protection, context (i.e., old town, urban areas, extra-urban areas, or isolated areas), density of the area, building position (i.e., isolated building, or building that is part of a block of several buildings), building sides facing the adjacent area (i.e., 1, 2, 3, all, or none), building distance from the main road inside the adjacent area (i.e., <5.00 m, 5.00–10.00 m, 10.00–20.00 m, >20.00 m, or absent), proximity to public spaces, and connections to the primary or secondary infrastructure network.

The *specific information* (Fig. S3) that was collected to assess the building vulnerability both in case of a tsunami and/or earthquake is: number of storeys above ground (i.e., 1, 2, 3, or absent), number of storeys below ground (i.e., 1, 2, or absent), storey height (i.e., <2.50 m, 2.50–3.50 m, 3.50–5.00 m, or >5.00 m), material of lateral resisting system (i.e., reinforced concrete, reinforced or unreinforced masonry with bricks or local stones/blocks, timber panels and timber frame, steel sheets and steel frame, other, or absent), foundation strength, shape of building footprint, seawall height and shape, source of large movable objects, brick wall around building, natural barriers, nearby suitable areas in case of emergency (i.e., adjacent area, portion of a street, or absent), and access to nearby suitable areas in case of emergency (i.e., easy, difficult, or no access). Further information related exclusively to the seismic vulnerability was also collected: presence/absence of tie-bars, roof material (i.e., reinforced concrete slabs, tiles on timber beams/joists ceiling, timber boards on timber beams/joists ceiling, metal sheets on timber beams/joist ceiling, metal sheets on steel beams/joist ceiling, other or absent), and roof type (i.e., double-pitched roof, mono-pitched roof, flat roof, barrel roof, or absent). Likewise, information related specifically to the tsunami vulnerability was collected: percentage of lateral surface with openings at the ground floor (i.e., 0–10%, 10–50%, or >50%), building position above the sea level (i.e., 1–10 m a.s.l., 10–20 m a.s.l., or >20 m a.s.l.), proximity to the coastline, and hypothetical impact of the waves on the structure (i.e., direct, indirect, partial, or none).

3.2. Analysing the historical evolution of urban and extra-urban settlements

To clarify the construction period of buildings, high-resolution aerial and satellite images in chronological sequence were compared (multi-temporal analysis). Starting from the 1950s aerial orthophoto up to the most recent satellite orthophoto, all territorial transformations were mapped in relation to the local evolutionary dynamics that occurred in the last seventy years. Moreover, considering the paucity of technical details on each structure (e.g., plans, sections, etc.), the multi-temporal analysis allowed validating information obtained through the rapid visual survey and relating each building to its specific materials and local construction techniques. As construction techniques represent the intangible heritage (i.e., [42–44] of a place, which is related to the local identity, non-structured interviews to some bricklayers were carried out to deeply know the peculiarities of both ancient and recent Aeolian buildings. Therefore, multi-temporal analysis together with non-structured interviews (social research field), allowed properly integrating information in the proposed survey-sheet model in the Stromboli case study.

The map of the historical evolution of urban and extra-urban settlements (Fig. 5a and b) was realised using three main high-resolution input data (details in Table 2): ancient IGMI-G.A.I. orthophoto of 1954 (i.e., OFC 1954_10 k, owned by DST-UNIFI), intermediate orthophoto of 1974 (i.e., OFC 1974_10 k, owned by DST-UNIFI) and PLÉIADES-1 satellite orthophoto of 8th October 2019 (i.e., PLEIADÉS-1 2019, owned by DST-UNIFI; see Ref. [68] for image details), supported by the use of Sicilian Region Technical Map (i.e., CTR 2013_10 k) and Google Earth Pro satellite image data.

The digital maps were realised at a 1:2000 scale of analysis according to the resolution of available input data, surface extension of the case study, and typology of cartographic representation. Although the accuracy and high detail level are two important requirements for this kind of map, sometimes it was necessary to simplify the digital procedure in order to have a good cartographic rendering in terms of readability of both buildings and roads.

This process started from the reproduction of settlements at the ancient historical threshold (i.e., 1954, Fig. 3a), then it continued through the reproduction of the elements at the intermediate (i.e., 1974) and recent historical ones (i.e., 2019, Fig. 3b), showing its progressive physical transformations (e.g., new construction, transformation, demolition without reconstruction, etc.). The CTR

Table 2
Input data used to realise the maps of the historical evolution of urban and extra-urban settlements on Stromboli Island.

Case study	Input Data	File format	Resolution
Stromboli	OFC 1954_10 k	raster	2 m × 2 m
	OFC 1974_10 k	raster	2 m × 2 m
	PLÉIADES-1 2019	raster	0.5 m × 0.5 m
	CTR 2013_10 k	vector	–

represented the base to start the digitization process: the information contained therein was corrected and completed not only through the comparison with orthophotos but also through direct observations during field surveys.

3.3. Assessing the relative risk

The refinement of a risk analysis of buildings exposed to geo-environmental hazards, such as earthquakes or tsunamis, must be consistent with the scale used for the analyses, territorial context, and territorial dynamics. Indeed, the approaches to address the relative risk assessment can be qualitative, quali-quantitative, or quantitative [34,71]) in relation to the available data.

For seismic risk analysis at a regional scale, Whitman et al. [73] propose a qualitative methodology based on damage probability matrices (DPM), which relate the intensity of the event to the most probable degree of structural damage. These matrices, which differ one from another according to the type of building, provide for a preliminary building classification related to the constructive characteristics as building typology, material, or load-bearing structure. Calvi et al. [10] propose a quantitative methodology based on a specific mechanical model, that allows predicting the effects of an earthquake on structures, according to the elastic response spectrum: the more detailed the scale of analysis is, the more sophisticated the model is, and then it requires specific information on structures and/or construction techniques building-by-building. Instead, the INGV/GNDT – National Group for Earthquake Defence (INGV/GNDT – Gruppo Nazionale per la Difesa dai Terremoti) suggests a regional-scale methodology based on the calculation of a vulnerability index [23]. The index relates the intensity of a seismic event to the degree of damage to buildings, through structural calculations and identification of all those factors that are responsible for the seismic response. The index calculation is linked to the analysis of building conditions and on-site retrieval of detailed information through a specific survey-sheet model, after that an earthquake occurred [23,24]. Quantitative methodologies, with a predominantly heuristic approach (because they are unrelated to direct observation of post-earthquake damage), are for example those proposed by the working groups of the Federal Emergency Management Agency (FEMA) [35] within the HAZUS methodological frameworks (e.g., Ref. [27] and used at an urban or regional scale. Regardless of the prediction of damage degree to structures, the vulnerability index is calculated considering the construction characteristics that most influence the building resistance to earthquakes of a given intensity. HAZUS frameworks usually define the seismic action on a building, considering the elastic response spectra to acceleration and displacement, the structural strength, and the inter-floor drift. The methodology used by Ref. [32] introduces the INSPIRE relative risk index, based on the HAZUS fragility curves and a survey-sheet model created to collect relevant building data.

To estimate the relative risk of buildings exposed to tsunami hazards Papathoma et al. [46,47] proposed a quali-quantitative methodology based on the PTVA model, implemented by Dall'Osso et al. [16,17]. The PTVA index is the result of the product of many indicators (i.e., construction material, number of storeys, ground floor hydrodynamics, foundation strength, building row, and natural or artificial barriers around the building), and it quantifies the relative risk of buildings to a tsunami wave. According to a quali-quantitative assessment of the relative risk of buildings through the PTVA and considering the absence of any specific fragility curves, the engineering characteristics of buildings (as well as the peculiarities of the immediate surroundings and territorial context) assume an important role to evaluate their performances.

In this work, relative risk assessment of buildings exposed to seismic or tsunami hazards, based on a quali-quantitative approach, consisted of: 1) the calculation of the INSPIRE index, associated with their construction characteristics and PGA, in case of earthquakes; 2) the calculation of the PTVA index, associated to their construction characteristics and the expected water level at their location, in case of tsunamis.

The hazard scenario proposed by INGV [61] was considered, in the event that an earthquake occurs on Stromboli Island or nearby. Therefore, the scenario, which is characterised by moderate-high intensities (I3), was simulated. At the same time, the hazard scenarios suggested by Fornaciai et al. [28,29] were examined, in the event that a tsunami occurs following submarine or subaerial landslides of the Sciara del Fuoco. In our work, we used scenario 1 related to a submarine landslide of 17.6×10^6 m^3, which is characterised by intensities from low (I1) to high (I4), and scenario 2 related to a subaerial landslide of 35.3×10^6 m^3, which is characterised by intensities from low (I1) to high (I4).

3.3.1. Adopted relative seismic risk index

The INSPIRE index (I_V) of each building on Stromboli island is calculated with the equation proposed by Gentile et al. [32]; which is composed of a baseline score (I_{BL}) and a performance modifier (ΔI_{PM}):

$$I_V = I_{BL} + \Delta I_{PM}$$

The baseline score depends on the probability of exceeding the life-safety damage state (P_{HAZUS}), for a user-selected value of PGA, calculated on the lognormal fragility curves available in the HAZUS-MH framework [27]. Those are defined based on four main parameters: building material (*Mat*), basic structural system (*BSS*), seismic design level (*Code*), building height (*Height*), and PGA. More details to define such parameters are provided in Gentile et al. [32]. Depending on such parameters, the HAZUS framework provides their median (μ) and dispersion (β), while the fragility functions are defined as follows:

$$P_{HAZUS}(Mat,\ BSS,\ Code,\ Height,\ PGA) = \Phi\left(\frac{ln\ PGA/\mu}{\beta}\right),\ i = 1:4$$

The I_{BL} index, defined in the range 0–50%, is defined by normalising the P_{HAZUS} based on the maximum and minimum fragility, for the same selected PGA level, across the entire HAZUS fragility database:

The ΔI_{PM} depends on eight secondary parameters, which are not directly considered in the calculation of baseline score but, if present, can compromise the seismic performance of the analysed building. Such parameters are: preservation condition, plan shape,

storey height uniformity, added storeys, infills at ground storey, short column, pounding, and unfavourable soil. Gentile et al. [32] provide the details to assign a score to each secondary parameter ($SCORE_i$). The ΔI_{PM}, which is usually scaled in the range 0–50%, is defined as a weighted sum of each of these scores, where w_i is the weight of parameter i (also provided in the above reference):

$$\Delta I_{PM} = \frac{1}{2}\sum_{i=1}^{8} w_i SCORE_i$$

Stromboli and Ginostra are characterised by buildings with different materials, number of storeys, foundation strength, preservation condition, etc. (see also [6,7]. For example, the most common local building typologies (i.e., Aeolian houses), generally associated with traditional construction techniques, could also show subsequently-added, more-recent building portions. Some other buildings were affected by changes in the number of storeys, and/or the general building conformation and shape.

The relevant attributes to compute the INSPIRE index were retrieved for each building on the island. It is worth mentioning, however, that it was not possible to find detailed information about most secondary modifiers, apart from the "preservation condition", which was the only one adopted.

3.3.2. Adopted relative tsunami risk index

The PTVA index of buildings was calculated considering the construction characteristics, the immediate surrounding, and the geographical location of every building. In this case, the equation proposed by Dall'Osso et al. [17] was applied:

Table 3
Principal constructive characteristics of buildings on Stromboli Island.

BUILDINGS				
FEATURES	Type A	Type B	Type C	Type D
Height	Storeys above ground: 1-2. Storey height (average): 3.50–5.00 m for main buildings; secondary buildings may have lower heights (2.50–3.50 m or < 2.50 m)	Storeys above ground: 1-2. Storey height (average): 2.50–3.50 m for main buildings; secondary buildings may have lower heights (<2.50 m).	Storeys above ground: 1. Storey height (average): 2.50–3.50 m or < 2.50 m.	Storeys above ground: 1. Storey height (average): 2.50–3.50 m or < 2.50 m.
Construction period	First half of the 1900s or earlier.	Second half of the 1900s or earlier *[vertical structure subtype 2]* Contemporary *[vertical structure subtype 1]*	Second half of the 1900s or earlier.	Second half of the 1900s or earlier.
Material of lateral load resisting system & vertical structure	Unreinforced masonry with local blocks/stones. Lime or cement-based plaster are used.	*Subtype 1* Reinforced concrete. Lime or cement-based plaster are used. *Subtype 2* Reinforced masonry with bricks or local blocks/stones. Lime or cement-based plaster are used.	*Subtype 1* Unreinforced masonry with brick or local blocks/stones. Lime or cement-based plaster are used. *[roof subtype A, B, or C]* *Subtype 2* Timber panel & timber frame. *[roof subtype B]* *Subtype 3* Steel sheet & steel frame. *[roof subtype C]*	*Subtype 1* Masonry colonnade with local block/ stone. *[roof subtype A]* *Subtype 2* Timber frame. *[roof subtype B]* *Subtype 3* Steel frame. *[roof subtype C or D]*
Roof structure	Wattle, local stones, lapilli, and lime on timber joist ceiling.	Reinforced concrete slab, usually.	*Subtype A* Timber boards on timber beams or joist ceiling. *Subtype B* Metal sheet on timber beams or joist ceiling. *Subtype C* Metal sheet on steel beams or joist ceiling.	*Subtype A* Timber joist ceiling. *Subtype B* Timber boards on timber joist ceiling. *Subtype C* Metal sheet on timber joist ceiling. *Subtype D* Metal sheet on steel joist ceiling.
Ground-floor openings	10–50% of opened ground-floor surfaces, for main buildings; secondary buildings may have 0–10% of opened ground-floor surfaces.	10–50% of opened ground-floor surfaces, for main buildings; secondary buildings may have 0–10% of opened ground-floor surfaces.	0–10% or 10–50% of opened ground-floor surfaces.	>50% of opened ground-floor surfaces.
Completeness	Completed.	Completed. Under construction or uncompleted, in some cases.	Completed.	Completed.
State of maintenance	High quality. Low quality or abandoned (e.g., ruins), in some cases.	High quality. Low quality or abandoned (e.g., uncompleted), in some cases	High quality. Low quality or abandoned, in some cases.	High quality. Low quality or abandoned, in some cases.

$$PTVA_{[1,5]} = \frac{2}{3}\left(SV_{[1,5]}\right) + \frac{1}{3}\left(WV_{[1,5]}\right)$$

The main characteristics used to define the index are the "structural vulnerability" (*SV*) and the "structural vulnerability in case of water intrusion" (*WV*). Both parameters are defined in the range 1–5. *SV* depends on building vulnerability (*Bv*), building surroundings (*Surr*), and exposure (*Ex*):

$$SV_{[1,125]} = Bv_{[1,5]} Surr_{[1,5]} Ex_{[1,5]}$$

Bv depends on six components: main construction material (*m*), number of storeys (*s*), ground floor hydrodynamics (*g*) foundation type (*f*), shape of building footprint and orientation (*so*), and preservation condition (*pc*). The index is defined as follows:

$$Bv_{[-1,\ +1]} = \frac{1}{409}\left(100 \cdot m + 85 \cdot s + 69 \cdot g + 69 \cdot f + 52 \cdot so + 34 \cdot pc\right)$$

Surr depends on five components: main construction material (*br*), number of storeys (*sw*), ground floor hydrodynamics (*nb*), foundation type (*mo*), and shape orientation (*w*). It is defined as follows:

$$Surr_{[-1,\ +1]} = \frac{1}{356}\left(100 \cdot br + 84 \cdot sw + 72 \cdot nb + 58 \cdot mo + 42 \cdot w\right)$$

For the Stromboli case study, it was not possible to find detailed information about the number of artificial barriers (e.g., dry-stone walls, brick and concrete walls, etc.) around buildings. Therefore, a value of 1 was assigned to the *w* factor for all the surveyed buildings.

The building exposure (*Ex*) depends on two components: the water depth above the terrain level at the building location, *WD*, and the maximum value of *WD* among all buildings exposed (WD_{max} WD). The *Wv* index depends on the water depth normalised by the building height. The two indices are defined as follows:

$$Ex_{[-1,\ +1]} = \frac{WD}{WD_{max}}$$

Fig. 4. The main constructive characteristics of buildings on Stromboli Island, summarised through four different types. In the figure, a) Type A, b) Type B, c) Type C, and d) Type D are reported.

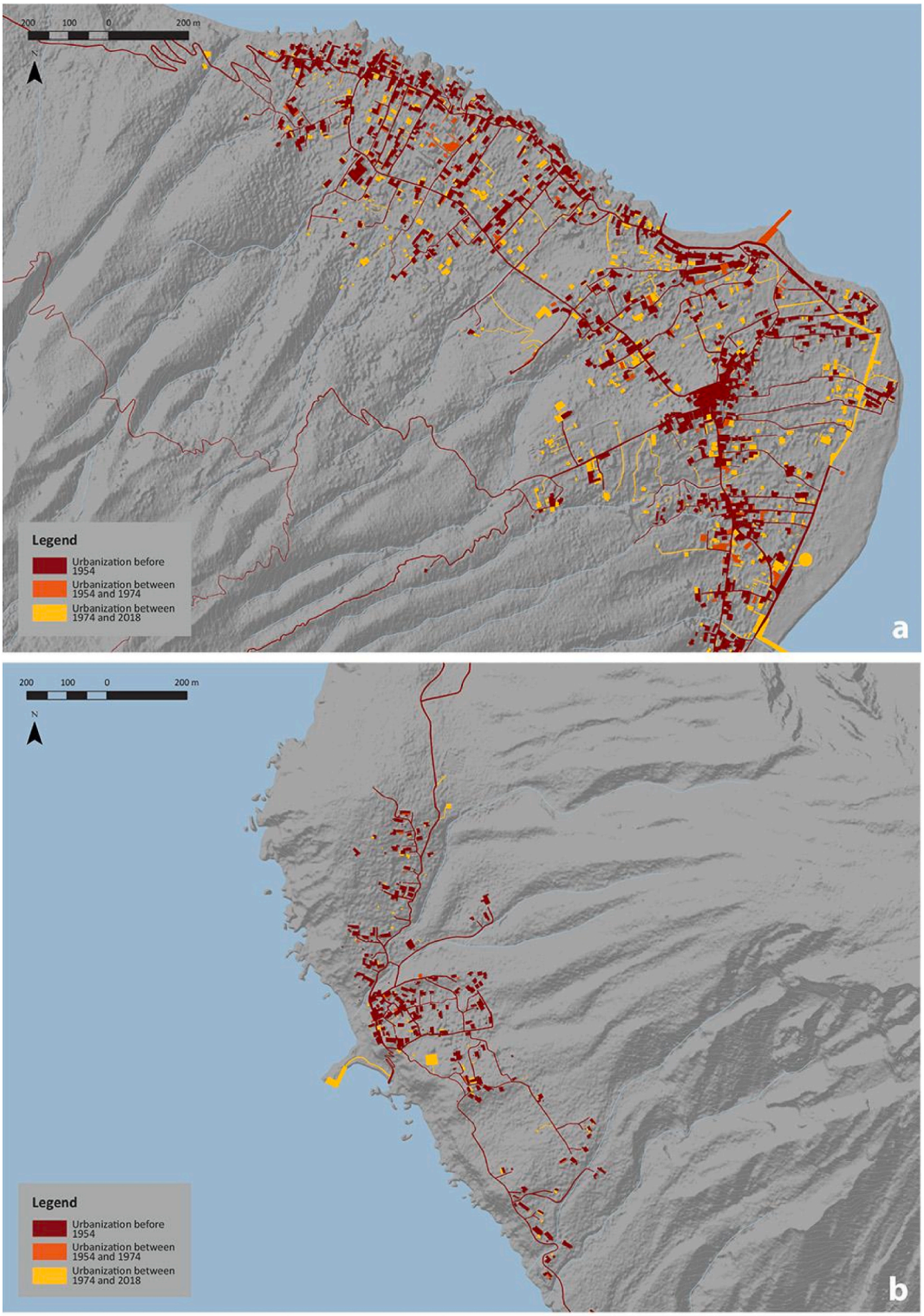

Fig. 5. Historical evolution of the urban and extra-urban settlements, in a) Stromboli village and b) Ginostra village.

$$Wv_{[0,1]} = \left(\frac{Height\ of\ inundated\ building\ levels}{Total\ height\ of\ building}\right)$$

The tsunami water depth at each building location is obtained based on the simulations by Refs. [28,29].

4. Results

4.1. Historical evolution of urban and extra-urban settlements

Stromboli shows a total of 2315 buildings, according to a mapping conducted by the authors between December 2018 and April 2019. The main construction characteristics of buildings are summarised in Table 3 and shown in Fig. 4.

Most of the Stromboli village was already present in the 1954 aerial orthophoto. It is considered the main anthropic persistence (i.e., [42–44] of the eastern side of the island because it retains its original Aeolian constructive characteristics: the urban core is located on the ancient site (since Late Neolithic, [5,54,74], near the San Vincenzo Ferreri church, while the extra-urban settlement consists of urban agglomerations along main inland roads or waterfront roads [2]. The ancient Aeolian buildings [2,14] show one or two floors above ground. The primary buildings, with an original residential function, have a storey height between 3.50 and 5.00 m ca., while the secondary buildings, with an original storehouse function, show a lower storey height between 2.50 and 3.50 m ca. or, in some cases, less than 2.50 m. According to the local construction techniques, they were usually constructed in unreinforced masonry (with local stones/blocks) and built without foundations. Their roof is always flat and consists of a composite slab made of wattle, local stones/lapilli, and lime on timber joists. Finally, the openings on the ground floor correspond to 10–50% of the total ground floor surface in the case of primary buildings, while it is generally <10% in the case of secondary buildings. As Alleruzzo Di Maggio [2] describes, the traditional houses are also composed of an external open space called "*bagghiu*", adjacent to the building and functional to the daily living activities of the Aeolian family. It is a specific type of "loggia", made of a masonry colonnade with local stones or blocks and a timber joist ceiling.

Between 1954 and 1978 buildings remained almost unchanged, both in terms of their spatial distribution and number. Between 1978 and 2019, buildings increased considerably, especially in Ficogrande, Punta Lena, and Scari along Marina Road (Via Marina), near the main harbour and very close to the pre-existing settlements of inland areas. The most recent buildings are related to the transformation of the local economy, increasingly based on seasonal tourism and less on traditional agro-silvo-pastoral activities or fishing, that characterised the Aeolian archipelago until the 1930s [2]. New construction and/or transformation of pre-existing buildings was carried out mainly to accommodate new tourists (e.g., hotels, b&b, apartments, info-point, etc.) or for commercial activities (e.g., bars, restaurants, shops, markets and supermarkets, etc.). The most-recent buildings show one or two floors above the ground, with a storey height ranging between 2.50 m and 3.50 m or, in some cases, less than 2.50 m regardless of their function. New buildings constructed in this period generally show a reinforced concrete lateral load resisting system and a reinforced concrete joist ceiling. If not completely new but recently transformed, they are usually made of reinforced masonry with bricks or local stone/blocks and a reinforced concrete joist ceiling. Also in this case, the openings on the ground floor correspond to 10–50% of the total ground floor surface in the case of primary buildings, while it is generally <10% in the case of secondary buildings.

Also, the most part of so-called 'light structures' (e.g. canopies and/or verandas) is recent and consists of timber frame with timber board on timber joist ceiling or steel frame with metal sheet on timber or steel joist ceiling.

In Ginostra village, all buildings remained reasonably unchanged from 1954 until today, and their constructive characteristics are the same as the ancient buildings of Stromboli village.

4.2. Calculated seismic and tsunami indices

The calculated seismic and tsunami indices obtained for Stromboli are summarised in Table 4. The calculated values of both indices were reclassified into four equivalent intervals to obtain relative risk classes (Figs. 6 and 7): R1 low (<25%), R2 moderate-low (26%–50%), R3 moderate-high (51%–75%), and R4 high (76%–100%). It is worth mentioning that it was impossible to collect detailed information for a small number of buildings, due to a lack of free access to private properties. For those buildings, it was therefore

Table 4
Relative seismic and tsunami risk indices on Stromboli Island.

BUILDING RELATIVE RISK										
Earthquakes	**R1**		**R2**		**R3**		**R4**		**Undefined**	
	n.	**%**	**n.**	**%**	**n.**	**%**	**n.**	**%**	**n.**	**%**
2315 assessed buildings	1029	44	1169	51	0	0	0	0	117	5
Tsunamis (scenario 1)	**R1**		**R2**		**R3**		**R4**		**Undefined**	
	n.	**%**	**n.**	**%**	**n.**	**%**	**n.**	**%**	**n.**	**%**
142 assessed buildings (with non-zero index)	67	47	64	45	4	3	0	0	7	5
Tsunamis (scenario 2)	**R1**		**R2**		**R3**		**R4**		**Undefined**	
	n.	**%**	**n.**	**%**	**n.**	**%**	**n.**	**%**	**n.**	**%**
309 assessed buildings (with non-zero index)	109	35	176	57	9	3	0	0	15	5

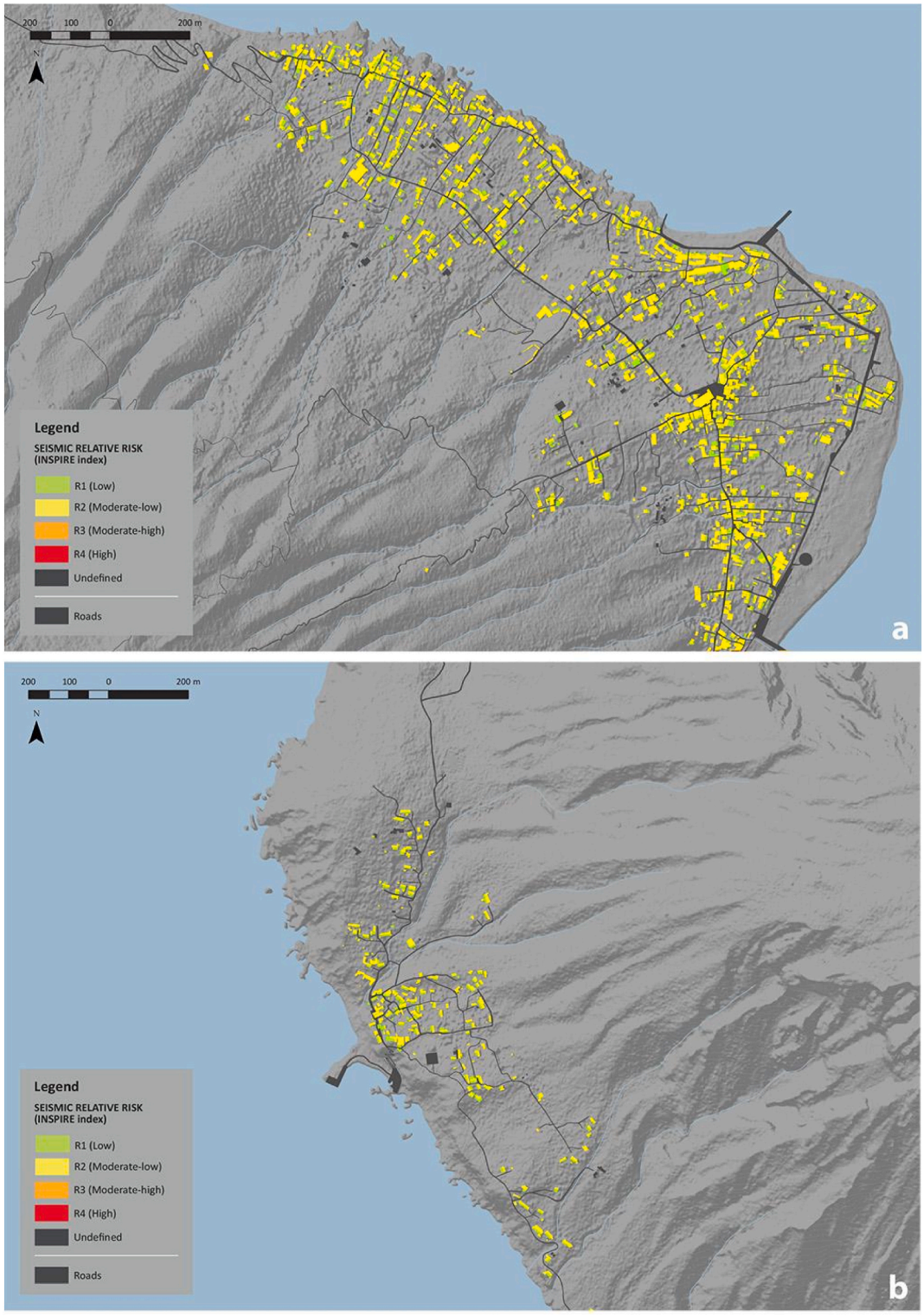

Fig. 6. Relative risk of buildings exposed to seismic hazard in a) Stromboli village and b) Ginostra village.

impossible to calculate the relative risk indices.

Concerning an earthquake scenario with PGA equal to 0.225 g, there are overall 2315 exposed buildings on Stromboli island: 44% are in the R1 class, 51% pertain to R2, while 5% are in the undefined class (i.e., no data available on the constructive characteristics of

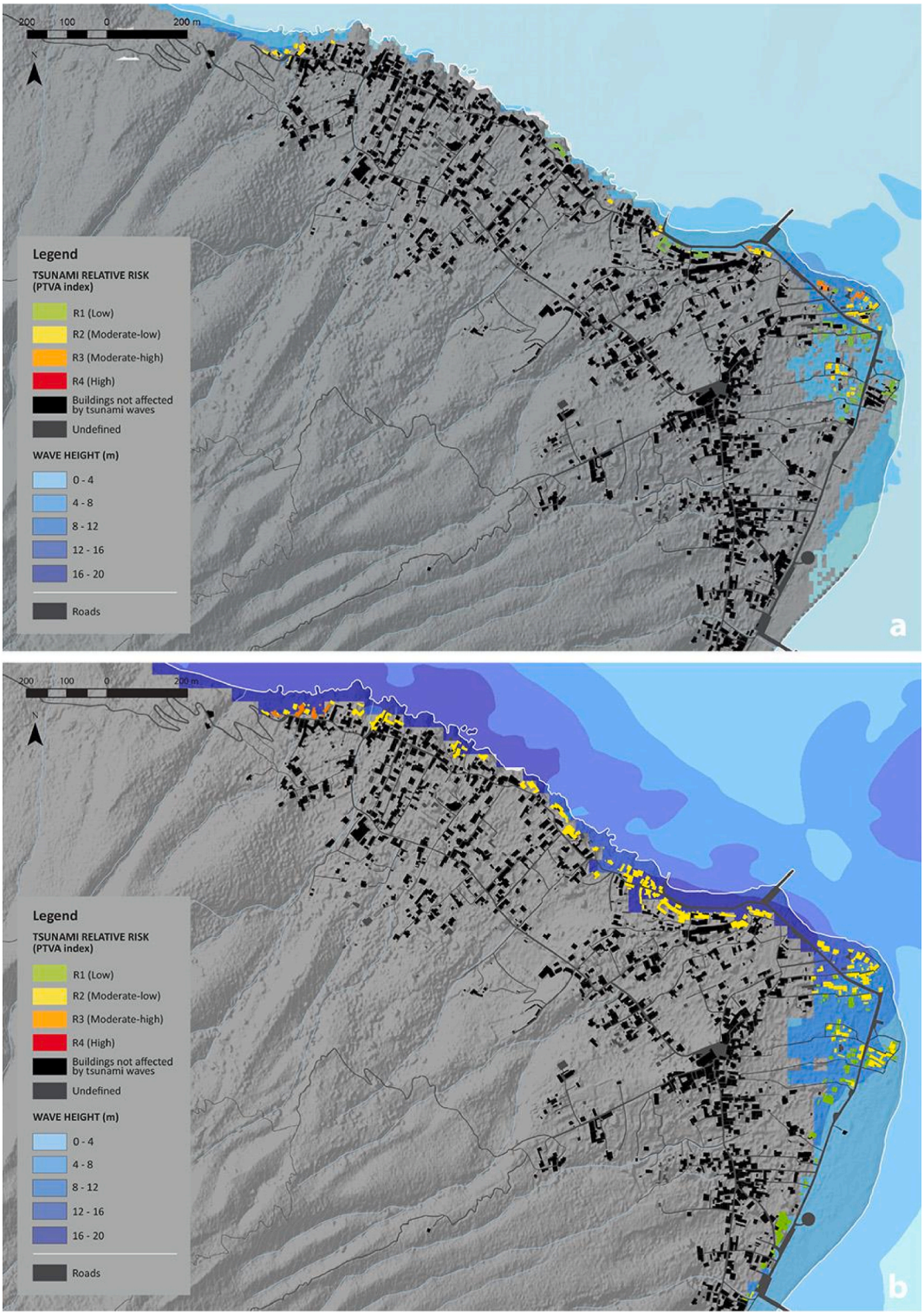

Fig. 7. Relative risk of buildings exposed to tsunami hazard in Stromboli village: a) scenario 1 (submarine landslide, 17.5×10^6 m^3) and b) scenario 2 (submarine landslide, 35.3×10^6 m^3).

buildings). Most likely, this is due to the particularly-low value of the PGA. The buildings pertaining to class R1 mainly refer to the so-called fixed or removable 'light buildings', regardless of their construction period. The primary and secondary buildings pertaining to class R2 mainly include the ancient ones with original Aeolian constructive characteristics and the recent ones which were subjected to

transformations.

As shown in Fig. 6a and b, the distribution of buildings in classes R1 and R2 are homogeneous throughout the island.

Considering the scenario 1 related to tsunami hazard (i.e., tsunami triggered by a submarine landslide of 17.5×10^6 m^3), there are overall 142 exposed buildings (i.e., with tsunami index greater than zero): 47% are in R1 class, 45% in R2 class, 3% in R3 class, while 5% are in the undefined class (i.e., no data available on the constructive characteristics of buildings). For scenario 2 (i.e tsunami triggered by an aerial landslide of 35.3×10^6 m^3), with a higher runup, the exposed buildings are equal to 309: 35% are in R1 class, 57% in R2 class, 3% in R3 class, while 5% are in the undefined class (i.e., no data available on the constructive characteristics of buildings).

As shown in Fig. 7a and b, the buildings exposed to tsunami hazards are located mainly in the north-eastern part of the island, with particular reference to Piscità, Ficogrande, and Scari. This result is valid for both the considered scenarios. Obviously, the waves triggered by an aerial landslide of 35.3×10^6 m^3 impact the coast of Piscità and Ficogrande more significantly than a wave triggered by a submarine landslide of 17.6×10^6 m^3. In both scenarios, the buildings with the highest relative risk are the ancient ones with the original Aeolian constructive characteristics, except for the 'light buildings'. The primary and secondary buildings vary from the R1 to the R3 relative risk class for scenario 1, while they range between R2 and R3 for scenario 2. In Scari, most of the exposed buildings are recent or recently transformed, with the exception of some ancient buildings in the extra-urban agglomerations close to the coast. For those, the relative risk class ranges between R1 and R2 for scenario 1. For scenario 2, the risk class of those buildings is more homogeneous and mostly falls into class R2.

5. Discussion

The present research aims at defining a prioritisation methodology, based on a relative estimation of risk for buildings in volcanic islands, such as Stromboli, which are not only affected by volcanic events but also by seismic and tsunami hazards. This procedure combines a quali-quantitative analysis for the assessment of building relative risk indices (i.e., [16,17,32] with the historical-geographical analysis of urban and extra-urban settlements, derived from the 'territorialist' approach (according to Refs. [42–44]. Therefore, considering the historical processes and socio-cultural models that influenced the anthropic settlements in terms of physical elements (e.g., buildings), construction techniques (e.g., materials, building typologies), and organisation of urban and extra-urban spaces allows analysing the relative risk of buildings in a holistic way. The historical-geographical analysis of the urban and extra-urban settlements was crucial because it allowed studying the geographical context over time, from both the physical evolutionary and transformative point of view. The site-specific inspections and field surveys, carried out using the herein-proposed survey-sheet model, were decisive because they allowed collecting data used to assess the relative risk on a building-by-building basis. Moreover, the survey-sheet model allowed comparing the data obtained on the field with the cartographic representation in Fig. 5, in order to correct and/or update the official cartographic data.

The proposed methodology shows that earthquakes and tsunamis have a different impact on Stromboli Island, not only in terms of the number of exposed buildings but also in terms of the relative risk index values, which are related to their vulnerability and the adopted scenario-based hazard footprints.

As reported in the historical chronicles and estimated by hazard maps, the expected seismic intensity on Stromboli is fairly low and homogeneous. Indeed, the relative seismic index is low (class R1) or moderate-low (class R2) for primary and secondary buildings, which mainly include the ancient ones with original Aeolian constructive characteristics (built in the first half of the 1900s or earlier), while it is generally low for the so-called fixed or removable 'light buildings' (mainly built in the second half of the 1900s).

For both the considered tsunami scenarios, there is a higher variability of the relative tsunami risk index, from low (class R1) to moderate-high (class R3), on the north-eastern coast of the island (i.e., Piscità, Ficogrande, and Scari). The qualitative distribution of the results is consistent with both the considered scenarios, which differ for their estimated runup. On Stromboli Island, buildings affected by tsunamis are mainly the primary and secondary ancient buildings, and the more recent 'light' buildings.

The literature describing the impact of the 2002 tsunami on Stromboli Island [30,45,66] offers the opportunity to compare the building relative risk calculated using scenario 1 and the damage detected on the Stromboli village a few days after the event. This work shows that in Piscità there is a cluster of buildings, particularly close to the north/north-western oriented coast, which are classified as moderate-low (class R2) tsunami relative risk index (Fig. 7a). This is in accordance with the observations reported by Tinti et al. [66]; describing the damage that occurred in Piscità as the collapse of small walls, balustrades, doors, and windows, without any structural damage to the buildings. Some objects and small boats were washed away and sand was accumulated inside the buildings and along the roads. Another small cluster of buildings in Ficogrande shows a moderate-low (class R2) to moderate-high (class R3) relative tsunami risk index. Fornaciai et al. [30] showed that all the buildings overlooking the beach are potentially hit by waves and that the old pier did not guarantee any protection. Tinti et al. [66] describe the damage that occurred in Ficogrande as severe. Many walls and some small constructions were demolished. Sand and gravel were accumulated by the waves in the courtyards, on the terraces, and inside the houses. In addition, the tsunami removed every object found on its path as volcanic rocks, boats, and scooters, which were then accumulated in the courtyards or along the roads. The biggest cluster of buildings with a moderate-low (class R2) to moderate-high (class R3) relative tsunami risk index is located close to Punta Lena (Fig. 7a), in accordance with the observation reported by Tinti et al. [65,66]; describing relevant damage as boundary wall demolished, gates, doors and windows destroyed, and fence and/or railing bend. The waves threw pebbles against buildings and some of them were trapped inside the grooves of several windows. The smallest pebbles were instead thrown on the building's roof up to 7 m high. The tsunami waves dragged small boats, home appliances, gas bottles and vegetation and, once the water retired, the furniture of several houses was chaotically piled up. In Scari, minor damage was observed and the tsunami waves also reached the power plant located at a distance of about 134 m from the

coastline.

The methodology adopted within this paper is affected by limitations. The scale of analysis, ranging between 1:10000, 1:5000, and 1:2000, considerably influenced the detail of historical-geographical analysis that was functional to validate the collected field data. The simplifications adopted in mapping the historical evolution of the settlements produced errors related to the cartographic rendering (e.g. the perimeter of some buildings was not identified correctly).

Moreover, the digitalisation procedure introduced interpretation errors depending on the resolution of the available images. On the one hand, the most recent aerial orthophoto (i.e., OFC 1974_10 K) and the PLEIADÉS-1 satellite orthophoto (i.e., PLEIADÉS-1 2019) are characterised by a high-resolution. On the other hand, the old IGMI-G.A.I. aerial orthophoto (OFC 1954_10 k) is characterised by a lower quality due to the orthorectification process. Another factor that influenced the completeness and accuracy of the digital procedure is the use of outdated CTR. The particularly-old Sicilian Region Technical Map (i.e., CTR 2013_10 k) does not provide enough information about the most recent buildings. Consequently, it was necessary to update the CTR using information acquired through the recent orthophotos and data obtained during field surveys.

The building-sheet model was created before the field surveys, intersecting two pre-existing models (i.e., AeDES and DST-UNIFI sheets). These models, used to analyse buildings at a local scale, are particularly detailed and require specific information on a case-by-case basis. Therefore, some simplifications were introduced to adapt the model to the required analysis scale and the large number of involved buildings.

Finally, a degree of error is implied by the uncertainty involved in assigning the surveyed buildings to a set of building classes identified in the literature for Stromboli island.

6. Conclusions

This paper proposed an innovative prioritisation methodology for buildings, based on estimating relative risk indices for earthquakes and tsunamis. The method envisages the identification/collection of information on the main compositional characteristics of buildings through a newly-developed survey-sheet model. Using historical-geographical analysis of the settlements, according to the 'territorialist' approach to the urban and regional planning and design, the method also allows integrating information on the built environment and better estimating the relative risk within a building portfolio.

The proposed method is applied to Stromboli Island, which is subject to seismic and tsunami hazards. The relative seismic risk of buildings within the island is fairly low and spatially uniform. Regarding tsunamis, the method improved previously-available results for Stromboli, identifying buildings with a higher relative risk index on the northern coast of the island and considering two tsunami scenarios: one related to a 17.6×10^6 m^3 submarine landslide; one related to a 35.3×10^6 m^3 subaerial landslide. Both scenarios confirm that the older buildings on the island are relatively more at risk than the 'light' newer buildings. Moreover, the spatial distribution of the tsunami indices is considerably more variable with respect to the seismic one.

With the appropriate modifications, the proposed method is applicable for other case-study areas affected by earthquakes and tsunamis, thus providing for a multi-hazard risk assessment perspective.

Author contribution

Conceptualization: A.T., F.D.T.; data analysis: A.T., R.G.; investigation and methodology: A.T., F.D.T., R.G.; writing – original draft preparation: A.T., F.D.T.; writing – review and editing: I.Z., R.G., R.F. All authors have read and agreed to the published version of the manuscript.

Declaration of competing interest

The authors declare that they have no known competing financial interests or personal relationships that could have appeared to influence the work reported in this paper.

Acknowledgments

This work has been partially supported by the "Presidenza del Consiglio dei Ministri – Dipartimento della Protezione Civile" (Presidency of the Council of Ministers – Department of Civil Protection); However, this publication does not reflect the position and the official policies of the Department (WP 3.2 "Modelling slope instability at the Stromboli volcano"; Scientific Responsibility: F.D.T.). The authors are particularly grateful to PINO, Carlo Lanza, Massimiliano Cincotta, and Salvatore Zaia for the logistic support during field surveys. Thanks also to Teresa Nolesini for the valuable contribution during field surveys.

Appendix A. Supplementary data

Supplementary data to this article can be found online at https://doi.org/10.1016/j.ijdrr.2022.103002.

References

[1] V. Acocella, M. Neri, P. Scarlato, Understanding shallow magma emplacement ar volcanoes: orthogonal feeder dikes during the 2002-2003 Stromboli (Italy) eruption, Geophys. Res. Lett. 33 (17) (2006).

[2] M.T. Alleruzzo Di Maggio, La casa rurale nelle Isole Eolie, in: CNR – Consiglio Nazionale Delle Ricerche (1975). *La casa Rurale Nella Sicilia Orientale* vol. 30, Leo S. Olschki Editore, Firenze, 1975, pp. 111–136. Ricerche Sulle Dimore in Italia.

[3] S. Arrighi, M. Rosi, J.C. Tanguy, V. Courtillot, Recent eruptive history of Stromboli (Aeolian Islands, Italy) determined from high-accuracy archeomagnetic dating, Geophys. Res. Lett. 31 (19) (2004).

[4] A. Bertagnini, P. Landi, The Secche di Lazzaro pyroclastics of Stromboli volcano: a phreatomagmatic eruption related to the Sciara del Fuoco sector collapse, Bull. Volcanol. 58 (2–3) (1996) 239–245.

[5] M. Bettelli, V. Cannavò, A. Di Renzoni, F. Ferranti, S.T. Levi, L'età del Bronzo a Stromboli: il villaggio terrazzato di San Vincenzo come avamposto nord-orientale dell'arcipelago eoliano. L'età del Bronzo a Stromboli: il villaggio terrazzato di San Vincenzo come avamposto nord-orientale dell'arcipelago eoliano, Scienze dell'Antichità 22 (2) (2016) 297–313.

[6] S. Biass, C. Bonadonna, F. Di Traglia, M. Pistolesi, M. Rosi, P. Lestuzzi, Probabilistic evaluation of the physical impact of future tephra fallout events for the Island of Vulcano, Italy, Bull. Volcanol. 78 (5) (2016) 37.

[7] S. Biass, J.L. Falcone, C. Bonadonna, F. Di Traglia, M. Pistolesi, M. Rosi, P. Lestuzzi, Great Balls of Fire: a probabilistic approach to quantify the hazard related to ballistics—a case study at La Fossa volcano, Vulcano Island, Italy, J. Volcanol. Geoth. Res. 325 (2016) 1–14.

[8] A. Bonaccorso, S. Calvari, G. Garfì, L. Lodato, D. Patanè, Dynamics of the December 2002 flank failure and tsunami at Stromboli volcano inferred by volcanological and geophysical observations, Geophys. Res. Lett. 30 (18) (2003).

[9] S. Calvari, F. Giudicepietro, F. Di Traglia, A. Bonaccorso, G. Macedonio, N. Casagli, Variable magnitude and intensity of Strombolian explosion: focus on the eruptive processes for a first classification scheme for Stromboli Volcano (Italy), Rem. Sens. 13 (5) (2021) 944–974.

[10] G.M. Calvi, R. Pinho, G. Magenes, J.J. Bommer, L.F. Restrepo- Vélez, H. Crowley, Development of seismic vulnerability assessment methodologies over the past 30 years, ISET J. Earthq. Technol. 43 (2006) 75–104.

[11] D. Casalbore, F. Passeri, P. Tommasi, L. Verrucci, A. Bosman, C. Romagnoli, F.L. Chiocci, Small-scale slope instability on the submarine flanks of insular volcanoes: the case-study of the Sciara del Fuoco slope (Stromboli), Int. J. Earth Sci. 109 (2020) 2643–2658.

[12] C. Cavallaro, Il terremoto di Stromboli del 16 aprile 1960, Riv. "Stromboli" 9 (1964) 3–15.

[13] F.L. Chiocci, C. Romagnoli, P. Tommasi, A. Bosman, The Stromboli 2002 tsunamigenic submarine slide: characteristics and possible failure mechanisms, J. Geophys. Res. Solid Earth 113 (B10) (2008).

[14] S. Colajanni, A. Lanza Volpe, La casa eoliana: un sistema di raffrescamento passivo. AGATHÓN. RCAPIA, PhD, Journal. Recupero dei Contesti Antichi e Processi Innovativi nell'Architettura, Università degli Studi di Palermo, Dipartimento di Architettura – Sezione: Progetto e Costruzione 1 (2012) 67–70.

[15] L. D'Auria, F. Giudicepietro, M. Martini, M. Orazi, The April-May 2006 Volcano-Tectonic Events at Stromboli Volcano (Southern Italy) and Their Relation with the Magmatic System, Istituto Nazionale di Geofisica e Vulcanologia, Rome, 2006. Earth Prints Repository, http://hdl.handle.net/2122/1506.

[16] F. Dall'Osso, A. Maramai, L. Graziani, B. Brizuela, A. Cavalleti, M. Gonnella, S. Tinti, Applying and validating the PTVA-3 Model at the Aeolian Island, Italy: assessment of the vulnerability of buildins to tsunamis, Nat. Hazards Earth Syst. Sci. 10 (2010) 1547–1562.

[17] F. Dall'Osso, D. Dominey-Howes, C. Tarabotto, D. Summerhayes, G. Withycombe, Revision and improvement of the PTVA-3 model for assessing tsunami building vulnerability using "international expert judgment": introducing the PTVA-4 model, Nat. Hazards 83 (2016) 1229–1256.

[18] A. Di Roberto, M. Rosi, A. Bertagnini, M.P. Marani, F. Gamberi, Distal Turbidites and Tsunamigenic Landslides of Stromboli Volcano (Aeolian Islands, Italy). Submarine Mass Movements and Their Consequences, Springer, Dordrecht, 2010, pp. 719–731.

[19] A. Di Roberto, A. Bertagnini, M. Pompilio, M. Bisson, Pyroclastic density currents at Stromboli volcano (Aeolian Islands, Italy): a case study of the 1930 eruption, Bull. Volcanol. 76 (2014) 827.

[20] F. Di Traglia, S. Bartolini, E. Artesi, T. Nolesini, A. Ciampalini, D. Lagomarsino, J. Martí, N. Casagli, Susceptibility of intrusion-related landslides at volcanic islands: the Stromboli case study, Landslides 15 (1) (2018) 21–29.

[21] F. Di Traglia, A. Fornaciai, M. Favalli, T. Nolesini, N. Casagli, Catching geomorphological response to volcanic activity on steep slope volcanoes using multi-platform remote sensing, Rem. Sens. 12 (3) (2020) 438–461.

[22] F. Di Traglia, A. Fornaciai, D. Casalbore, M. Favalli, I. Manzella, C. Romagnoli, F.L. Chiocci, P. Cole, T. Nolesini, N. Casagli, Subaerial-submarine morphological changes at Stromboli volcano (Italy) induced by the 2019–2020 eruptive activity, Geomorphology (2022) 108093, https://doi.org/10.1016/j.geomorph.2021.108093.

[23] Inventario e vulnerabilità degli edifici pubblici e strategici dell'Italia centro-meridionale, in: M. Dolce, A. Martinelli (Eds.), Analisi di vulnerabilità e rischio sismico, INGV/GNDT Istituto Nazionale di geofisica e Vulcanologia/Gruppo Nazionale per la Difesa dai Terremoti II –, 2005, pp. 1–187.

[24] M. Dolce, F. Papa, A.G. Pizza, in: Manuale per la compilazione della scheda di 1° livello di rilevamento danno, pronto intervento e agibilità per edifici ordinari nell'emergenza postsismica (AeDES), PCM – DPCM, 2014, pp. 1–121.

[25] T. Esposti Ongaro, M. de'Micheli Vitturi, M. Ceraminara, A. Fornaciai, L. Nanniperi, M. Favalli, B. Calusi, J. Macìas, M.J. Castro, S. Ortega, J.M. Gonzàlez-Vida, C. Escalante, Modeling tsunamis generated by submarine landslides at Stromboli Volcano (Aeolian Islands, Italy): a numerical benchmark study, Front. Earth Sci. 9 (2021) 1–21.

[26] S. Falsaperla, S. Spampinato, Tectonic seismicity at Stromboli volcano (Italy) from historical data and seismic records, Earth Planet Sci. Lett. 173 (1999) 425–437.

[27] FEMA – Federal Emergency Management Agency, Hazus Earthquake Model. Technical Manual, 4.2, HAZUS, Washington DC, 2020, pp. 1–436. SP.

[28] A. Fornaciai, M. Favalli, L. Nanniperi, Numerical simulation of the tsunamis generated by the sciara del Fuoco landslides (Stromboli island, Italy), Sci. Rep. 9 (1) (2019) 1–12.

[29] A. Fornaciai, M. Favalli, L. Nanniperi, Author Correction: numerical simulation of the tsunamis generated by the sciara del Fuoco landslides (Stromboli island, Italy), Sci. Rep. 11 (1) (2021) 1–9.

[30] A. Fornaciai, M. Favalli, L. Nanniperi, Reconstruction of the 2002 Tsunami at Stromboli Using the Non-hydrostatic WAVE Model (NHWAVE), Geologicaal Society, London, 2021, p. 519. Special Publication.

[31] L. Francalanci, F. Lucchi, J. Keller, G. De Astis, C.A. Tranne, Eruptive, volcano-tectonic and magmatic history of the Stromboli volcano (north-eastern Aeolian archipelago), Geol. Soc. Lond. Mem. 37 (1) (2013) 397–471.

[32] R. Gentile, C. Galasso, From rapid visual survey to multi-hazard risk prioritisation and numerical fragility of school buildings in Banda Aceh, Indonesia, Nat. Hazards Earth Syst. Sci. 19 (2019) 1365–1386.

[33] G. Giordano, M. Porreca, P. Musacchio, M. Mattei, The Holocene Secche di Lazzaro phreatomagmatic succession (Stromboli, Italy): evidence of pyroclastic density current origin deduced by facies analysis and AMS flow directions, Bull. Volcanol. 70 (10) (2008) 1221–1236.

[34] M.S. Kappes, M. Keiler, K. von Elverfeldt, T. Glade, Challenges of analysing multi-hazard risk: a review, Nat. Hazards 64 (2012) 1925–1958.

[35] C.A. Kircher, R.V. Whitman, W.T. Holmes, HAZUS earthquake loss estimation methods, Nat. Hazards Rev. 7 (2006) 45–59.

[36] P. Kokelaar, C. Romagnoli, Sector collapse, sedimentation and clast population evolution at an active island-arc volcano: Stromboli, Italy, Bull. Volcanol. 57 (4) (1995) 240–262.

[37] M. Locati, R. Camassi, A. Rovida, E. Ercolani, F. Bernardini, V. Castelli, C.H. Caracciolo, A. Tertulliani, A. Rossi, R. Azzaro, S. D'Amico, S. Conte, E. Rocchetti, A. Antonucci, Italian Macroseismic Database (DBMI15), Version 2.0, National Institute of Geophysics and Volcanology (INGV), 2019, https://doi.org/10.13127/DBMI/DBMI15.2.

[38] M.F. Loreto, G. Pagnoni, F. Pettenati, A. Armigliato, S. Tinti, D. Sandron, F. Brutto, F. Muto, L. Facchin, F. Zgur, Reconstructed seismic and tsunami scenarios of the 1905 Calabria earthquake (SE Tyrrhenian sea) as a tool for geohazard assessment, Eng. Geol. 224 (2017) 1–14.

[39] F. Lucchi, L. Francalanci, G. De Astis, C.A. Tranne, E. Braschi, M. Klaver, Geological evidence for recurrent collapse-driven phreatomagmatic pyroclastic density currents in the Holocene activity of Stromboli volcano, Italy, J. Volcanol. Geoth. Res. 385 (2019) 81–102.
[40] G. Ma, F. Shi, J.T. Kirby, Shock-capturing nonhydrostatic model for fully dispersive surface wave processes, Ocean Model. 43 (2012) 22–35.
[41] G. Ma, J.T. Kirby, F. Shi, Numerical simulation of tsunami waves generated by deformable submarine landslides, Ocean Model. 69 (2013) 146–165.
[42] A. Magnaghi, Una metodologia analitica per la progettazione identitaria del territorio, in: A. Magnaghi (Ed.), Rappresentare i luoghi. Metodi e tecniche, Alinea Editrice, Firenze, 2001, pp. 1–40, 2001.
[43] A. Magnaghi, Il Progetto Locale, Bollati Boringhieri, Torino, 2010, pp. 1–313.
[44] A. Magnaghi, Draft of the Territorialists' Society Manifesto, SDT – Società dei Territorialisti/e ONLS, 2011, pp. 1–8.
[45] A. Maramai, L. Graziani, S. Tinti, Tsunamis in the aeolian Islands (southern Italy): a review, Mar. Geol. 215 (1–2) (2005) 11–21.
[46] M. Papathoma, D. Dominey-Howes, Tsunami vulnerability assessment and its implications for coastal hazard analysis and disaster management planning, Gulf of Corinth, Greece, Nat. Hazards Earth Syst. Sci. 3 (2003) 722–747.
[47] M. Papathoma, D. Dominey-Howes, Y. Zong, D. Simith, Assessing tsunami vulnerability, an example from Herakleio, Crete, Nat. Hazards Earth Syst. Sci. 3 (2003) 377–389.
[48] V. Pazzi, S. Morelli, F. Pratesi, T. Sodi, L. Valori, L. Gambaccini, N. Casagli, Assessing the safety of schools affected by geo-hydrologic hazards: the geohazard safety classification (GSC), Int. J. Disaster Risk Reduc. 15 (2016) 80–93.
[49] C.M. Petrone, E. Braschi, L. Francalanci, Understanding the collapse–eruption link at Stromboli, Italy: a microanalytical study on the products of the recent Secche di Lazzaro phreatomagmatic activity, J. Volcanol. Geoth. Res. 188 (4) (2009) 315–332.
[50] M. Pistolesi, A. Bertagnini, A. Di Roberto, M. Ripepe, M. Rosi, Tsunami and tephra deposits record interactions between past eruptive activity and landslides at Stromboli volcano, Italy, Geology 48 (5) (2020) 436–440.
[51] A. Riccò, Riassunto della sismografia del terremoto calabro siculo del 16 novembre, 1894, Rend. della R. Accad. dei Lincei VIII (3–12) (1899) 35–45.
[52] G. Risica, F. Speranza, G. Giordano, G. De Astis, F. Lucchi, Palaeomagnetic dating of the Neostromboli succession, J. Volcanol. Geoth. Res. 371 (2019) 229–244.
[53] C. Romagnoli, D. Casalbore, F.L. Chiocci, A. Bosman, Offshore evidence of large-scale lateral collapses on the eastern flank of Stromboli, Italy, due to structurally-controlled, bilateral flank instability, Mar. Geol. 262 (1–4) (2009) 1–13.
[54] M. Rosi, S.T. Levi, M. Pistolesi, A. Bertagnini, D. Brunelli, V. Cannavò, A. Di Renzoni, F. Ferranti, A. Renzulli, D. Yoon, Geoarchaeological evidence of middle-age tsunamis at Stromboli and consequences for the tsunami hazard in the Southern Tyrrhenian Sea, Sci. Rep. 9 (1) (2019) 1–10.
[55] L.N. Schaefer, F. Di Traglia, E. Chaussard, Z. Lu, T. Nolesini, N. Casagli, Monitoring volcano slope instability with Synthetic Aperture Radar: a review and new data from Pacaya (Guatemala) and Stromboli (Italy) volcanoes, Earth Sci. Rev. 192 (2019) 236–257.
[56] L. Schambach, S.T. Grilli, D.R. Tappin, M.D. Gangemi, G. Barbaro, New simulations and understanding of the 1908 Messina tsunami for a dual seismic and deep submarine mass failure source, Mar. Geol. 421 (2020) 106093.
[57] J. Selva, S. Lorito, M. Volpe, F. Romano, R. Tonini, P. Perfetti, F. Bernardi, M. Taroni, A. Scala, A. Babeyko, F. Løvholt, S.J. Gibbond, J. Macías, M.J. Castro, J. M. Gonzales-Vida, C. Sànchez-Linares, H.B. Bayraktar, R. Basili, F.E. Maesano, M.M. Tiberti, F. Mele, A. Piatanesi, A. Amato, Probabilistic tsunami forecasting for early warning, Nat. Commun. 12 (1) (2021) 1–14.
[58] R.J.S. Spence, P.J. Baxter, G. Zuccaro, Building vulnerability and human casualty estimation for a pyroclastic flow: a model and its application to Vesuvius, J. Volcanol. Geoth. Res. 133 (2004) 321–343.
[59] R.J.S. Spence, G. Zuccaro, S. Petrazzuoli, P.J. Baxter, Resistance of buildings to pyroclastic flows: analytical and experimental studies and their application to vesuvius, Nat. Hazards Rev. 4 (2004) 48–50.
[60] F. Speranza, M. Pompilio, F. D'Ajello Caracciolo, L. Sagnotti, Holocene eruptive history of the Stromboli volcano: constraints from paleomagnetic dating, J. Geophys. Res. Solid Earth 113 (B9) (2008).
[61] M. Stucchi, C. Meletti, V. Montaldo, A. Akinci, E. Faccioli, P. Gasperini, L. Malagnini, G. Valensise, Pericolosità sismica di riferimento per il territorio nazionale MPS04 [Data set], Istituto Nazionale di Geofisica e Vulcanologia (INGV), 2004, https://doi.org/10.13127/sh/mps04/ag.
[62] A. Tibaldi, Multiple sector collapses at Stromboli volcano, Italy: how they work, Bull. Volcanol. 63 (2–3) (2001) 112–125.
[63] A. Tibaldi, C. Corazzato, M. Marani, F. Gamberi, Subaerial-submarine evidence of structures feeding magma to Stromboli Volcano, Italy, and relations with edifice flank failure and creep, Tectonophysics 469 (1–4) (2009) 112–136.
[64] S. Tinti, A. Manucci, G. Pagnoni, A. Armigliato, F. Zaniboni, The 30 December 2002 landslide-induced tsunamis in Stromboli: sequence of the events reconstructed from the eyewitness accounts, Nat. Hazards Earth Syst. Sci. 5 (2005) 763–775.
[65] S. Tinti, A. Maramai, A. Armigliato, L. Graziani, A. Manucci, G. Pagnoni, F. Zaniboni, Observation of physical effects from tsunamis of December 30, 2002 at Stromboli volcano, southern Italy, Bull. Volcanol. 68 (2006) 450–461.
[66] S. Tinti, G. Pagnoni, F. Zaniboni, The landslides and tsunamis of the 30th of December 2002 in Stromboli analysed through numerical simulations, Bull. Volcanol. 68 (5) (2006) 462–479.
[67] P. Tommasi, P. Baldi, F.L. Chiocci, M. Coltelli, M. Marsella, M. Pompilio, C. Romagnoli, The Landslide Sequence Induced by the 2002 Eruption at Stromboli Volcano. Landslides, Springer, Heidelberg, Germany, 2005, pp. 251–258.
[68] A. Turchi, F. Di Traglia, T. Luti, D. Olori, I. Zetti, R. Fanti, Environmental aftermath of the 2019 Stromboli eruption, Rem. Sens. 12 (6) (2020) 994.
[69] S. Valade, G. Lacanna, D. Coppola, M. Laiolo, M. Pistolesi, D. Delle Donne, R. Genco, E. Marchetti, G. Ulivieri, C. Allocca, C. Cigolini, T. Nishimura, P. Poggi, M. Ripepe, Tracking dynamics of magma migration in open-conduit systems, Bull. Volcanol. 78 (2016) 78.
[70] L. Verrucci, P. Tommasi, D. Boldini, A. Graziani, T. Rotonda, Modelling the instability phenomena on the NW flank of Stromboli Volcano (Italy) due to lateral dyke intrusion, J. Volcanol. Geoth. Res. 371 (2019) 245–262, vicente.
[71] R. Vicente, S. Parodi, S. Lagomarsino, H. Varum, J.A.R. Mendes Silva, Seismic vulnerability and risk assessment: case study of the historic city centre of Coimbra, Portugal, Bull. Earthq. Eng. 9 (2011) 1067–1096.
[72] T.R. Walter, R. Wang, V. Acocella, M. Neri, H. Grosser, J. Zschau, Simultaneous magma and gas eruptions at three volcanoes in southern Italy: an earthquake trigger? Geology 37 (3) (2009) 251–254.
[73] R.V. Whitman, J.W. Reed, S.T. Hong, Earthquake damage probability matrices, Rome, in: Proceedings of the 5th World Conference on Earthquake Engineering, 1974, p. 2531.
[74] W. Zhao, E. Forte, S.T. Levi, M. Pipan, G. Tian, Improved high-resolution GPR imaging and characterization of prehistoric archaeological features by means of attribute analysis, J. Archaeol. Sci. 54 (2015) 77–85.
[75] G. Zuccaro, F. Cacace, R.J.S. Spence, P.J. Baxter, Impact of explosive eruption scenarios at Vesuvius, J. Volcanol. Geoth. Res. 178 (2008) 416–453.
[76] G. Zuccaro, M. Dolce, D. De Gregorio, E. Speranza, C. Moroni, La scheda CARTIS per la caratterizzazione tipologico-strutturale dei comparti urbani costituiti da edifici ordinari. Valutazione dell'esposizione in analisi di rischio sismico. Atti del 34° Convegno Nazionale 2015, Sessione 2.3, GNGTS Repository, 2015.